Published in final edited form as:
Neuroscience. 2010 June 2; 167(4): 1249–1256. doi:10.1016/j.neuroscience.2010.02.078.

CENTRAL AUTONOMIC REGULATION IN CONGENITAL CENTRAL HYPOVENTILATION SYNDROME

Jennifer A. Ogren[1], **Paul M. Macey**[1,2], **Rajesh Kumar**[3], **Mary A. Woo**[1], and **Ronald M. Harper**[2,3,*]

Dr. Miles Herkenham
Bethesda, MD, USA.

[1]UCLA School of Nursing, Los Angeles, California 90095

[2]Brain Research Institute, University of California at Los Angeles, Los Angeles, California 90095

[3]Department of Neurobiology, David Geffen School of Medicine at UCLA, Los Angeles, California 90095

Abstract

Congenital central hypoventilation syndrome (CCHS) patients show significant autonomic dysfunction in addition to the well-described loss of breathing drive during sleep. Some characteristics, e.g., syncope, may stem from delayed sympathetic outflow to the vasculature; other symptoms, including profuse sweating, may derive from overall enhanced sympathetic output. The dysregulation suggests significant alterations to autonomic regulatory brain areas. Murine models of the genetic mutations present in the human CCHS condition indicate brainstem autonomic nuclei are targeted; however, the broad range of symptoms suggests more widespread alterations. We used functional magnetic resonance imaging (fMRI) to assess neural response patterns to the Valsalva maneuver, an autonomic challenge eliciting a sequence of sympathetic and parasympathetic actions, in nine CCHS and 25 control subjects. CCHS patients showed diminished and time-lagged heart rate responses to the Valsalva maneuver, and muted fMRI signal responses across multiple brain areas. During the positive pressure phase of the Valsalva maneuver, CCHS responses were muted, but were less so in recovery phases. In rostral structures, including the amygdala and hippocampus, the normal declining patterns were replaced by increasing trends or more modest declines. Earlier onset responses appeared in the hypothalamus, midbrain, raphé pallidus, and left rostral ventrolateral medulla. Phase-lagged responses appeared in cerebellar pyramis and anterior cingulate cortex. The time-distorted and muted central responses to autonomic challenges likely underlie the exaggerated sympathetic action and autonomic dyscontrol in CCHS, impairing cerebral autoregulation, possibly exacerbating neural injury, and enhancing the potential for cardiac arrhythmia.

[*]**Correspondence to:** Ronald M. Harper, Ph.D. Distinguished Professor Department of Neurobiology David Geffen School of Medicine at UCLA University of California at Los Angeles Los Angeles, CA 90095-1763, USA rharper@ucla.edu Tel: 310-825-5303 Fax: 310-825-2224.

Keywords

Valsalva maneuver; sleep; sympathetic; limbic; insula; cerebellum

Congenital central hypoventilation syndrome (CCHS) is a rare condition associated with mutation of the paired-like homeobox PHOX2B gene (Amiel et al., 2003), and shows principal characteristics of diminished breathing drive during sleep and impaired ventilatory sensitivity to CO_2 and O_2; those characteristics constantly impose a burden for maintaining vital function (American Thoracic Society, 1999). However, CCHS is also accompanied by impaired autonomic regulation, which is manifested as profuse sweating (Vanderlaan et al., 2004), loss of thermoregulation (American Thoracic Society, 1999), exaggerated responses to cold pressor challenges (Kim et al., 2002), lateralized pupillary dilation (Vanderlaan et al., 2004), diminished heart rate variation with respiration (Woo et al., 1992), and loss of nocturnal “dipping” of blood pressure (Trang et al., 2003). More severe cardiovascular symptoms include life-threatening periods of asystole and syncope. Asystole may underlie instances of sudden death in CCHS, necessitating cardiac pacing in some affected individuals (Gronli et al., 2008).

The extensive impaired autonomic characteristics in CCHS suggest a disrupted organization of function in the condition, resulting from altered axonal projections, cellular injury, or impaired interactions between central nervous sites that regulate autonomic action. Extensive axonal injury appears in CCHS (Kumar et al., 2005, Kumar et al., 2008, Kumar et al., 2009b, Kumar et al., 2010), and selected sites show altered functional magnetic resonance imaging (fMRI) signal responses to autonomic challenges (Macey et al., 2004a, Macey et al., 2005). Some of these sites show extensive tissue loss using structural MRI techniques, as shown by alterations in tissue water content, and changes in the diffusion of water through affected areas (Kumar et al., 2005, Macey et al., 2005, Kumar et al., 2006, 2008, Kumar et al., 2009a, Kumar et al., 2009b, Macey et al., 2009). Dilation of the basilar arteries in CCHS (Kumar et al., 2009c), and inappropriate global blood oxygen level dependent (BOLD) signals to O_2 and CO_2 challenges (Macey et al., 2003) suggest impaired regulation of the cerebral vasculature in the syndrome. Deficits in autonomic innervation to the cerebral vasculature have the potential to further exacerbate injury through inadequate perfusion during periods of enhanced energy demand.

The putative mechanism underlying CCHS, mutation of PHOX2B, plays a significant role in central nervous system cell differentiation (Pattyn et al., 1999, Amiel et al., 2003, Dauger et al., 2003). Areas demonstrated as targets of Phox2b mutations in mice include peripheral autonomic ganglia and medullary autonomic structures, such as the nucleus of the solitary tract (NTS), and specific sites near the parafacial nuclei mediating components of respiratory action (Stornetta et al., 2006, Dubreuil et al., 2008). Other brain areas which show structural injury in CCHS have not been typically identified as targets of PHOX2B expression, and have not been classically considered for roles in autonomic regulation affected in the condition. However, damage to the cerebellum, and more rostral brain injuries indicated by diffusion tensor imaging and T2-relaxometry techniques are extensive (Kumar et al., 2005, Kumar et al., 2006, 2008), and some of the autonomic regulation disturbed in CCHS depends on several of these sites for adequate function. The advent of the Allen Brain Atlas reveals that Phox2b expression is more widely spread than initially realized (Lein et al., 2007), raising the potential for injury in more diverse brain regions as a result of PHOX2B mutations, especially in rostral areas mediating many autonomic functions deficient in the syndrome.

The severe consequences of excessive and lateralized sympathetic outflow, which results in enhanced potential for arrhythmia (Oppenheimer et al., 1992), as well as modified cerebral perfusion, mandate examination of processes underlying autonomic dysfunction in CCHS. We hypothesized that activity in neural sites regulating autonomic influences would show patterns conducive to inappropriate or inadequate perfusion in CCHS patients, which may elicit further neural injury. Such impairments would also contribute to exaggerated sympathetic outflow and other autonomic coordination problems characteristic of autonomic dysfunction in CCHS. We examined fMRI signal responses of the entire brain in CCHS and control subjects during a sequence of Valsalva maneuvers, which elicit a pattern of sympathetic and parasympathetic responses. The objective was to determine brain areas recruited to the Valsalva challenge, and assess timing and magnitude of response patterns within autonomic regulatory areas that may differ in CCHS subjects.

EXPERIMENTAL PROCEDURES

Subjects

We studied nine CCHS patients (mean age ± SD: 20 ± 3 years, 7 male) and 25 healthy controls (mean age ± SD: 19 ± 4 years, 16 male). The diagnosis of CCHS was made based on American Thoracic Society criteria (American Thoracic Society, 1999). CCHS patients requiring ventilatory support while awake, and those diagnosed with other neurological injury or nervous system disorders, such as Hirschsprung's disease, were excluded from the study. Genotyping was only available for two subjects, who were both positive for PHOX2B mutations (expansions 20/25 and 20/27). Patients were recruited via the CCHS family network (http://www.cchsnetwork.org). Control subjects were free of any known cardiovascular or neurological disorder, and were recruited through posted advertisements on the university campus. An additional two CCHS subjects were recruited, but excluded as they were unable to complete the Valsalva maneuver; one could not seal the tracheostomy opening, and another could not reach the target pressure. Two additional control subjects were similarly excluded because they could not maintain the target pressure. All subjects and their parents/guardians gave written informed consent/assent prior to the study. The study protocol was approved by the Institutional Review Board at the University of California at Los Angeles.

Physiology/Valsalva maneuver

Subjects lay supine in the MRI scanner during a baseline period and subsequent performance of a sequence of four Valsalva maneuvers. All subjects remained awake during the entire scanning sequence, without sedation or anesthesia. During each challenge period, subjects were cued by a blue task light to exhale forcibly into a flexible tube until at least 30 mmHg pressure was reached, and to maintain this pressure for 17.5 seconds. The target pressure level was indicated to the subject by a green light. Expiratory load pressure, respiratory movements, and pulse oximetry were recorded. Each challenge was followed by a one-minute rest interval, and the last challenge was followed with a 110 s baseline.

Magnetic resonance imaging

Brain images were collected using a 3.0 Tesla MRI scanner (Siemens Magnetom, Tim-Trio, Erlangen, Germany), with an eight-channel receive-only phased-array head coil. Foam pads were placed on either side of the head to reduce motion artifact. During each sequence of four Valsalva maneuvers, 188 fMRI brain volumes were acquired using a spin-echo echo-planar imaging (EPI) sequence [repetition time (TR) = 2500 ms, echo-time (TE) = 30 ms, flip angle (FA) = 90°, matrix size = 90 × 90, field of view (FOV) = 230 × 230 mm, slice thickness = 3.6 mm, 43 slices]. For visual examination and structural identification, high-resolution T1-weighted images were acquired using a magnetization prepared rapid

acquisition gradient-echo (MPRAGE) pulse sequence (TR = 2200 ms; TE = 2.34 ms; inversion time = 900 ms; FA = 9°; matrix size = 320 × 320; FOV = 230 × 230 mm; slice thickness = 0.9 mm; 192 slices).

Data analysis

High-resolution T1-weighted images were visually assessed for any brain pathology. We used MATLAB (The MathWorks, Inc., Natick, MA), SPM5, SAS statistical software (The SAS Institute, Cary, NC; Littell, 2006), MRIcron (Rorden et al., 2007), and MATLAB-based custom software to analyze data.

Physiology—Each subject's respiratory signal, heart rate, and load pressure values during the challenge periods were examined to ensure proper performance of the Valsalva maneuvers. Heart rates were calculated from the raw signal acquired with the pulse oximeter. Group signals were assessed both as a continuous average across the entire period as well as averages across the four Valsalva maneuvers. Repeated measures analysis of variance (RMANOVA) was implemented in SAS using the “proc mixed” procedure (Littell, 2006), allowing determination of within-group responses relative to baseline, and between-group differences in response. The Tukey-Fisher criterion for multiple comparisons was used, i.e., the model variables of group, time, and group × time were assessed for overall significance (threshold $p = 0.05$) before investigating the model for specific time-points of response or group differences.

fMRI Preprocessing—The initial three of 188 volumes were excluded to allow for signal saturation. The remaining volumes were motion-corrected, adjusted for distortions using a phase-difference fieldmap (Hutton et al., 2002), bias corrected for field-related signal inhomogeneities and normalized to common space (Ashburner and Friston, 2005), and spatially smoothed (Gaussian filter kernel = 8 mm). A detrending procedure was used to correct for global effects (Macey et al., 2004b).

fMRI Cluster analysis—Cluster analysis was used to determine regions responding according to an *a priori*-defined pattern of response. Using the preprocessed images, signals were examined with a mixed-effects paradigm, using an on/off (boxcar) model during each challenge. The statistical parametric maps resulting from modeling the boxcar pattern of response were compared between groups using two-sample t-tests (uncorrected, $p < 0.01$), and clusters with significant differences were overlaid onto a background image derived from all subjects’ normalized T1-weighted images, for structural identification.

fMRI VOI analysis—Volume of interest (VOI) analysis was performed to determine the time course of responses in *a priori*-defined regions. Selected brain regions were defined according to SPM atlas-based toolboxes, including Automated Anatomical Labeling (AAL) (Tzourio-Mazoyer et al., 2002) and the Anatomy Toolbox (Eickhoff et al., 2005), and other VOI were manually traced. For each time point, the mean signal intensity was calculated across all voxels in the VOI. Changes in signal intensity relative to baseline were calculated and compared within and between CCHS and control groups using RMANOVA (see Physiology data analysis).

RESULTS

Physiology

All included subjects were able to achieve and maintain adequate load pressures to the Valsalva challenge. There were no significant differences between groups in time it took to achieve the minimum pressure (Fig. 1E). Control subjects, however, achieved higher mean

load pressure than CCHS patients during the challenge period ($p < 0.05$, RMANOVA). CCHS baseline heart rates were significantly higher (Fig. 1A; mean ± stdev: CCHS 81.3 ± 1.4 bpm, control 71.6, ± 1.3 bpm), and extent of change in heart rate during the challenge was lower (Fig. 1A, D). At onset of the pressure period, CCHS heart rate responses did not exhibit initial transients, as in controls, but dipped much lower below baseline, subsequently showed a slower rise time during the pressure period, and were slower to decline during recovery (Fig. 1D).

fMRI signals

Two approaches were used to assess the neural signals: a cluster analysis, indicating areas over the entire brain showing mean signal differences during the challenge, and a VOI analysis, which provided time trends over the sequence of Valsalva maneuvers. The cluster analysis revealed significant mean signal changes in multiple areas, as shown in Figure 2. The brain areas that showed significant changes included the hypothalamus, midbrain, mid-cingulate cortex, pons and medulla, including the ventrolateral medulla (VLM) and raphé (magnus, obscurus, and pallidus), thalamus, hippocampus, amygdala, insula, claustrum, basal ganglia, and cerebellar cortex. We used cluster analysis to identify additional autonomic regulatory sites to those chosen *a priori*, but since our primary interest was the patterning of fMRI signals, we focused on the VOI analysis of time-trends.

Response patterns: Controls—The response patterns are presented as averaged trends for separate areas. Time trends in the ventral cerebellum and insula for the sequence of Valsalva maneuvers, together with trends of averaged heart rate for each group, are shown in Figure 1. “On” and “off” transients appeared (Fig 3A). For most left-sided rostral brain areas, the dominant pattern during the positive pressure period was a declining signal. On the right side, however, a biphasic component appeared, with a dominant increasing signal, as shown by the hippocampus and amygdala (Fig. 3A, B). Caudal brain areas largely differed from rostral sites; rather than a declining signal in the positive pressure phase, after the initial transient, a unidirectional signal increase appeared, as in medullary sites (Fig. 4A). Right caudal cerebellar cortex sites showed a similar unidirectional response, but an inverse declining response on the left side during the positive pressure period (Fig. 4C). In the recovery phase, caudal areas typically showed a decline, followed by recovery to baseline (Fig. 4, 5C, D). During the recovery phase, signals were often biphasic in both rostral and caudal sites (Fig. 3-5).

Response patterns: CCHS—CCHS patterns typically differed within the positive pressure period of the Valsalva maneuver from controls, with the most remarkable characteristic being a profound muting of responses in a wide range of structures, with the most substantial differences appearing in the insulae and ventral cerebellum (Fig. 3C, 4C). Thalamic responses were virtually indistinguishable from those of the insulae. Signal muting was less pronounced in other areas, e.g., parabrachial pons and ventrolateral medulla (Fig. 4A, B). In a number of sites, control responses showed a pronounced lateralization of direction in signal change, i.e. increase vs decrease, but CCHS responses did not. Closer inspection revealed that the CCHS signal patterns showed no, or minimal declines, and less-affected increases, resulting in marked left-sided differences over controls, but less dramatic right-sided differences. This pattern was particularly noted in limbic areas such as the amygdala (Fig. 3A), where dampened left-sided declines contrasted with normal-magnitude right-sided increases in CCHS. In structures where control subjects showed symmetrical left and right responses, e.g., hypothalamus (Fig. 5B), the CCHS patients showed a similar pattern (Fig. 3D, 5A, B).

CCHS response time shifts relative to Control responses—The cingulate cortex and cerebellar pyramis response patterns differed from most sites, showing delayed timing in CCHS (Fig. 5A, C). The distribution of sites showing time-leads or time-lags indicated a significant proportion of structures were sited in the rostral brain, principally in limbic areas, and especially the hypothalamus (Fig. 3, 5B). Responses during the positive pressure period developed later in the anterior cingulate (Fig. 5A), and earlier in the hippocampus, amygdala, mammillary bodies, hypothalamus, ventrolateral medulla, raphé pallidus, midbrain, and ventral tegmental area (Fig. 3A, B, D; 4A; 5B-D). The phase shifts ranged from a 2.5 s lag to a 7.5 s lead.

DISCUSSION

Two findings were of special interest: 1) within specific neural structures, most responses to the Valsalva maneuver were muted in CCHS subjects compared with controls, and 2) timing of CCHS responses often preceded or lagged those of controls, and likely contributed to the time-distorted heart rate response following Valsalva release. The timing offsets, as well as the impaired extent of responses, may underlie many of the autonomic dysfunctions found in the syndrome, particularly the transient appearance of asystole and episodes of syncope, which depend on appropriate timing of sympathetic changes to a pressor challenge. Children with CCHS show a remarkably high incidence of prolonged QT intervals, with all children in one sample showing durations greater than standard cutoffs of 450 ms; QT intervals did not vary by genotype (Gronli et al., 2008).

Several aspects of the response patterns are of particular interest with respect to CCHS cardiovascular characteristics. The higher resting heart rate likely derived from the overall impaired parasympathetic action in the condition, as earlier demonstrated by diminished respiratory-related heart rate variation (Woo et al., 1992) and by impaired heart rate responses to a number of vagally-mediated breathing challenges (Kim et al., 2002, Macey et al., 2004c). The insular cortex, a principal area for autonomic regulation (Yasui et al., 1991), is normally lateralized in function, with sympathetic regulation largely on the right side, and parasympathetic regulation on the left (Oppenheimer et al., 1992, Oppenheimer et al., 1996, Zhang and Oppenheimer, 1997, Critchley et al., 2000). The insula exerts considerable influence on hypothalamic and medullary autonomic regulation, with damage potentially releasing normal inhibitory influences on those structures, resulting in significant autonomic signs or cardiovascular injury after stroke in humans (Oppenheimer and Hachinski, 1992, Colivicchi et al., 2004, Laowattana et al., 2006) and potentiation of arrhythmia after stimulation in animals (Oppenheimer et al., 1991). However, other brain areas may be involved in post-stroke cardiac events (Rincon et al., 2008). Both insular cortices show significant structural damage in CCHS, as measured by mean diffusivity (Kumar et al., 2006). The response of the CCHS right insula was virtually abolished in the positive pressure period of the Valsalva, and was muted in the release period. The diminished insular responses may result from the structural injury, and contribute to exaggerated sympathetic tone in the condition, increasing the likelihood of arrhythmia. The failure of the left insular signal to decline in the same fashion as controls may reflect another aspect of the impaired parasympathetic action in the syndrome. Structural damage also appears in the thalamus, cerebellum, midbrain, amygdala, hippocampus, mammillary body, caudate, and cingulate (Kumar et al., 2005, Kumar et al., 2006, 2008, Kumar et al., 2009a, Kumar et al., 2009b, Macey et al., 2009), which showed response deficits here and likely contribute to the functional impairments.

Limited signal declines in CCHS

Although signals in most structures were muted in CCHS patients relative to controls, the diminished extent of signal change appeared principally with decreasing signals; CCHS patients showed no, or minimal signal declines where control signals substantially declined. In some areas, the effect was so dramatic as to appear as a "signal inversion," e.g., mammillary bodies. The consequence of the signal phase change would effectively be an inverted influence of the structure, namely increased action when control structures would be diminishing influence. In the case of the mammillary bodies, which lose a substantial source of their axonal input from the hippocampus in CCHS (Kumar et al., 2009b, Macey et al., 2009), the descending influences to midbrain structures would exert inappropriate signals to brainstem and cerebellar areas.

Timing alterations

Selected areas showed an early development of signals in CCHS during the positive pressure period; this pattern was more common than time-delayed responses, and appeared in the amygdala, hippocampus, mammillary bodies, midline midbrain and ventral tegmental area, parabrachial pons, and left, but not right medulla. Of the neural structures affected, the cerebellum plays a significant coordination role in somatic motor acts; phase shifts in the cerebellar pyramis showed a delay, and the output pattern for the pyramis may be allowing the earlier emergence of responses in rostral structures. The manner in which the changes in timing develop remains unclear.

Time shifting of responses in CCHS has the potential to exert major effects on both parasympathetic and sympathetic regulation. Too-early suppression of vascular flow occurring while neural discharge increases could lead to excitotoxic injury, and exacerbate damage already present in the syndrome. Phase-lagged responses can lead to late vascular dilation or constriction, depending on structure. The consequences of inappropriate timing of sympathetic relative to parasympathetic control can be severe, since prolonged QT intervals can accompany unilateral excessive sympathetic outflow (Roden et al., 1996, Schwartz, 2006). Prolonged QT intervals, characteristic of CCHS, predispose to ventricular fibrillation and sudden death; sudden death is common in CCHS (Gronli et al., 2008, Weese-Mayer et al., 2009).

PHOX2B mutations

Early studies of PHOX2B expression focused on murine peripheral autonomic ganglia of the viscera and carotid bodies, and on medullary nuclei of the NTS (Stornetta et al., 2006), and areas near the parafacial nuclei (Dubreuil et al., 2008). However, expression is also high in cerebellar, hippocampal and hypothalamic regions, and appears in the globus pallidus, nucleus of the diagonal band, medial and lateral septum, anterior dorsal thalamus, midbrain, and portions of the amygdala (Lein et al., 2007). Expression of PHOX2B within these areas in humans is unknown, but all of these sites showed muted responses in CCHS, and most showed time-shifted patterns.

With evidence that more extreme forms of the mutation can be associated with sudden death (Gronli et al., 2008), we have continued to make repeated efforts to obtain genotyping on these subjects. For a number of reasons, parents and/or guardians have often been unwilling or unable to avail their children for this evaluation, and ethical considerations preclude mandating that they do so as a condition of study participation. Currently, we rely on physiological characteristics as the principal identifier. Our subjects showed remarkable consistency in the major physiological characteristics associated with CCHS; all showed early-onset symptoms, were ventilatory-dependent during sleep, demonstrated impaired CO_2

and O_2 ventilatory responses, and exhibited significant autonomic disturbances as reflected in cardiac variability, temperature regulation, sweating and pupillary responsiveness. However, the extent of certain autonomic perturbations did vary, possibly reflecting variation in mutation characteristics.

Conclusions

The findings emphasize that autonomic disturbances in CCHS most likely result from an impaired network of distributed brain structures mediating sympathetic and parasympathetic control, not just alterations to isolated brainstem nuclei as earlier suggested in animal models of Phox2b mutations. Responses to the Valsalva maneuver in CCHS patients are muted across widespread brain areas, are preferentially restricted on response decline, and are often early relative to control responses. The distorted nature of these responses, within structures critical for autonomic regulation, demonstrates the possibility for exacerbation of neural injury in the syndrome. The source of these injuries remains unclear, but possible mechanisms include cell differentiation problems secondary to initial PHOX2B issues, hypoxic exposure resulting from hypoventilation, or impaired cerebral perfusion resulting from early PHOX2B effects, potentially compounded by progressive autonomic dysregulation. The extent of PHOX2B expression in multiple brain areas that serve autonomic regulatory roles emphasizes the potential for mutations in that gene to contribute to wide-spread autonomic functional deficits in the condition. Phox2b expression in mice has now been shown in cerebellar, midbrain, diencephalic, and forebrain areas, where damage was once thought to result only from hypoxic processes. Although comparable expression in humans is not yet demonstrated, the primary effects of PHOX2B mutations are likely more widespread than initially realized in CCHS.

Acknowledgments

We thank Ms. Rebecca K. Harper, Ms. Christiane M. Abouzeid, Mr. Raymond Chong, and Mr. Edwin M. Valladares for assistance with data collection. This research was supported by the National Institute of Child Health and Human Development R01 HD-22695.

ABBREVIATIONS

CCHS	Congenital central hypoventilation syndrome
fMRI	Functional magnetic resonance imaging
BOLD	Blood oxygen level dependent
NTS	Nucleus of the solitary tract
EPI	Echo planar imaging
TR	Repetition-time
TE	Echo-time
FA	Flip angle
FOV	Field-of-view
MPRAGE	Magnetization prepared rapid acquisition gradient echo
RMANOVA	Repeated measures analysis of variance
AAL	Automated Anatomical Labeling
VOI	Volume of interest

ACC	Anterior cingulate cortex
VTA	Ventral tegmental area
VLM	Ventrolateral medulla

REFERENCES

American Thoracic Society. Idiopathic congenital central hypoventilation syndrome: diagnosis and management. Am J Respir Crit Care Med 1999;160:368–373. [PubMed: 10390427]

Amiel J, Laudier B, Attie-Bitach T, Trang H, de Pontual L, Gener B, Trochet D, Etchevers H, Ray P, Simonneau M, Vekemans M, Munnich A, Gaultier C, Lyonnet S. Polyalanine expansion and frameshift mutations of the paired-like homeobox gene PHOX2B in congenital central hypoventilation syndrome. Nat Genet 2003;33:459–461. [PubMed: 12640453]

Ashburner J, Friston KJ. Unified segmentation. Neuroimage 2005;26:839–851. [PubMed: 15955494]

Colivicchi F, Bassi A, Santini M, Caltagirone C. Cardiac autonomic derangement and arrhythmias in right-sided stroke with insular involvement. Stroke 2004;35:2094–2098. [PubMed: 15272134]

Critchley HD, Corfield DR, Chandler MP, Mathias CJ, Dolan RJ. Cerebral correlates of autonomic cardiovascular arousal: a functional neuroimaging investigation in humans. J Physiol 2000;523(Pt 1):259–270. [PubMed: 10673560]

Dauger S, Pattyn A, Lofaso F, Gaultier C, Goridis C, Gallego J, Brunet JF. Phox2b controls the development of peripheral chemoreceptors and afferent visceral pathways. Development (Cambridge, England) 2003;130:6635–6642.

Dubreuil V, Ramanantsoa N, Trochet D, Vaubourg V, Amiel J, Gallego J, Brunet JF, Goridis C. A human mutation in Phox2b causes lack of CO2 chemosensitivity, fatal central apnea, and specific loss of parafacial neurons. Proc Natl Acad Sci U S A 2008;105:1067–1072. [PubMed: 18198276]

Eickhoff SB, Stephan KE, Mohlberg H, Grefkes C, Fink GR, Amunts K, Zilles K. A new SPM toolbox for combining probabilistic cytoarchitectonic maps and functional imaging data. NeuroImage 2005;25:1325–1335. [PubMed: 15850749]

Gronli JO, Santucci BA, Leurgans SE, Berry-Kravis EM, Weese-Mayer DE. Congenital central hypoventilation syndrome: PHOX2B genotype determines risk for sudden death. Pediatr Pulmonol 2008;43:77–86. [PubMed: 18041756]

Hutton C, Bork A, Josephs O, Deichmann R, Ashburner J, Turner R. Image distortion correction in fMRI: A quantitative evaluation. Neuroimage 2002;16:217–240. [PubMed: 11969330]

Kim AH, Macey PM, Woo MA, Yu PL, Keens TG, Gozal D, Harper RM. Cardiac responses to pressor challenges in Congenital Central Hypoventilation Syndrome. Somnologie 2002;6:109–115.

Kumar R, Ahdout R, Macey PM, Woo MA, Avedissian C, Thompson PM, Harper RM. Reduced caudate nuclei volumes in patients with congenital central hypoventilation syndrome. Neuroscience 2009a;163:1373–1379. [PubMed: 19632307]

Kumar R, Lee K, Macey PM, Woo MA, Harper RM. Mammillary Body and Fornix Injury in Congenital Central Hypoventilation Syndrome. Pediatr Res 2009b;66:429–434. [PubMed: 19581831]

Kumar R, Macey PM, Woo MA, Alger JR, Harper RM. Elevated mean diffusivity in widespread brain regions in congenital central hypoventilation syndrome. J Magn Reson Imaging 2006;24:1252–1258. [PubMed: 17075838]

Kumar R, Macey PM, Woo MA, Alger JR, Harper RM. Diffusion tensor imaging demonstrates brainstem and cerebellar abnormalities in congenital central hypoventilation syndrome. Pediatr Res 2008;64:275–280. [PubMed: 18458651]

Kumar R, Macey PM, Woo MA, Alger JR, Keens TG, Harper RM. Neuroanatomic deficits in congenital central hypoventilation syndrome. J Comp Neurol 2005;487:361–371. [PubMed: 15906312]

Kumar R, Macey PM, Woo MA, Harper RM. Rostral brain axonal injury in congenital central hypoventilation syndrome. J Neurosci Res. 2010 DOI: 10.1002/jnr.22385.

Kumar R, Nguyen HD, Macey PM, Woo MA, Harper RM. Dilated basilar arteries in patients with congenital central hypoventilation syndrome. Neurosci Lett 2009c;467:139–143. [PubMed: 19822189]

Laowattana S, Zeger SL, Lima JA, Goodman SN, Wittstein IS, Oppenheimer SM. Left insular stroke is associated with adverse cardiac outcome. Neurology 2006;66:477–483. discussion 463. [PubMed: 16505298]

Lein ES, Hawrylycz MJ, Ao N, Ayres M, Bensinger A, Bernard A, Boe AF, Boguski MS, Brockway KS, Byrnes EJ, Chen L, Chen TM, Chin MC, Chong J, Crook BE, Czaplinska A, Dang CN, Datta S, Dee NR, Desaki AL, Desta T, Diep E, Dolbeare TA, Donelan MJ, Dong HW, Dougherty JG, Duncan BJ, Ebbert AJ, Eichele G, Estin LK, Faber C, Facer BA, Fields R, Fischer SR, Fliss TP, Frensley C, Gates SN, Glattfelder KJ, Halverson KR, Hart MR, Hohmann JG, Howell MP, Jeung DP, Johnson RA, Karr PT, Kawal R, Kidney JM, Knapik RH, Kuan CL, Lake JH, Laramee AR, Larsen KD, Lau C, Lemon TA, Liang AJ, Liu Y, Luong LT, Michaels J, Morgan JJ, Morgan RJ, Mortrud MT, Mosqueda NF, Ng LL, Ng R, Orta GJ, Overly CC, Pak TH, Parry SE, Pathak SD, Pearson OC, Puchalski RB, Riley ZL, Rockett HR, Rowland SA, Royall JJ, Ruiz MJ, Sarno NR, Schaffnit K, Shapovalova NV, Sivisay T, Slaughterbeck CR, Smith SC, Smith KA, Smith BI, Sodt AJ, Stewart NN, Stumpf KR, Sunkin SM, Sutram M, Tam A, Teemer CD, Thaller C, Thompson CL, Varnam LR, Visel A, Whitlock RM, Wohnoutka PE, Wolkey CK, Wong VY, Wood M, Yaylaoglu MB, Young RC, Youngstrom BL, Yuan XF, Zhang B, Zwingman TA, Jones AR. Genome-wide atlas of gene expression in the adult mouse brain. Nature 2007;445:168–176. [PubMed: 17151600]

Littell, RC. SAS for mixed models. SAS Institute, Inc.; Cary, N.C.: 2006.

Macey KE, Macey PM, Woo MA, Harper RK, Alger JR, Keens TG, Harper RM. fMRI signal changes in response to forced expiratory loading in congenital central hypoventilation syndrome. J Appl Physiol 2004a;97:1897–1907. [PubMed: 15258126]

Macey PM, Alger JR, Kumar R, Macey KE, Woo MA, Harper RM. Global BOLD MRI changes to ventilatory challenges in congenital central hypoventilation syndrome. Respir Physiol Neurobiol 2003;139:41–50. [PubMed: 14637309]

Macey PM, Macey KE, Kumar R, Harper RM. A method for removal of global effects from fMRI time series. NeuroImage 2004b;22:360–366. [PubMed: 15110027]

Macey PM, Macey KE, Woo MA, Keens TG, Harper RM. Aberrant neural responses to cold pressor challenges in congenital central hypoventilation syndrome. Pediatr Res 2005;57:500–509. [PubMed: 15718375]

Macey PM, Richard CA, Kumar R, Woo MA, Ogren JA, Avedissian C, Thompson PM, Harper RM. Hippocampal volume reduction in congenital central hypoventilation syndrome. PLoS One 2009;4:e6436. [PubMed: 19649271]

Macey PM, Valderama C, Kim AH, Woo MA, Gozal D, Keens TG, Harper RK, Harper RM. Temporal trends of cardiac and respiratory responses to ventilatory challenges in congenital central hypoventilation syndrome. Pediatr Res 2004c;55:953–959. [PubMed: 15028846]

Oppenheimer SM, Gelb A, Girvin JP, Hachinski VC. Cardiovascular effects of human insular cortex stimulation. Neurology 1992;42:1727–1732. [PubMed: 1513461]

Oppenheimer SM, Hachinski VC. The cardiac consequences of stroke. Neurol Clin 1992;10:167–176. [PubMed: 1557001]

Oppenheimer SM, Kedem G, Martin WM. Left-insular cortex lesions perturb cardiac autonomic tone in humans. Clin Auton Res 1996;6:131–140. [PubMed: 8832121]

Oppenheimer SM, Wilson JX, Guiraudon C, Cechetto DF. Insular cortex stimulation produces lethal cardiac arrhythmias: a mechanism of sudden death? Brain Res 1991;550:115–121. [PubMed: 1888988]

Pattyn A, Morin X, Cremer H, Goridis C, Brunet JF. The homeobox gene Phox2b is essential for the development of autonomic neural crest derivatives. Nature 1999;399:366–370. [PubMed: 10360575]

Rincon F, Dhamoon M, Moon Y, Paik MC, Boden-Albala B, Homma S, Di Tullio MR, Sacco RL, Elkind MS. Stroke location and association with fatal cardiac outcomes: Northern Manhattan Study (NOMAS). Stroke 2008;39:2425–2431. [PubMed: 18635863]

Roden DM, Lazzara R, Rosen M, Schwartz PJ, Towbin J, Vincent GM. Multiple mechanisms in the long-QT syndrome. Current knowledge, gaps, and future directions. The SADS Foundation Task Force on LQTS. Circulation 1996;94:1996–2012. [PubMed: 8873679]

Rorden C, Karnath HO, Bonilha L. Improving lesion-symptom mapping. J Cogn Neurosci 2007;19:1081–1088. [PubMed: 17583985]

Schwartz PJ. The congenital long QT syndromes from genotype to phenotype: clinical implications. J Intern Med 2006;259:39–47. [PubMed: 16336512]

Stornetta RL, Moreira TS, Takakura AC, Kang BJ, Chang DA, West GH, Brunet JF, Mulkey DK, Bayliss DA, Guyenet PG. Expression of Phox2b by brainstem neurons involved in chemosensory integration in the adult rat. J Neurosci 2006;26:10305–10314. [PubMed: 17021186]

Trang H, Boureghda S, Denjoy I, Alia M, Kabaker M. 24-hour BP in children with congenital central hypoventilation syndrome. Chest 2003;124:1393–1399. [PubMed: 14555571]

Tzourio-Mazoyer N, Landeau B, Papathanassiou D, Crivello F, Etard O, Delcroix N, Mazoyer B, Joliot M. Automated anatomical labeling of activations in SPM using a macroscopic anatomical parcellation of the MNI MRI single-subject brain. NeuroImage 2002;15:273–289. [PubMed: 11771995]

Vanderlaan M, Holbrook CR, Wang M, Tuell A, Gozal D. Epidemiologic survey of 196 patients with congenital central hypoventilation syndrome. Pediatr Pulmonol 2004;37:217–229. [PubMed: 14966815]

Weese-Mayer DE, Rand CM, Berry-Kravis EM, Jennings LJ, Loghmanee DA, Patwari PP, Ceccherini I. Congenital central hypoventilation syndrome from past to future: model for translational and transitional autonomic medicine. Pediatr Pulmonol 2009;44:521–535. [PubMed: 19422034]

Woo MS, Woo MA, Gozal D, Jansen MT, Keens TG, Harper RM. Heart rate variability in congenital central hypoventilation syndrome. Pediatr Res 1992;31:291–296. [PubMed: 1561018]

Yasui Y, Breder CD, Saper CB, Cechetto DF. Autonomic responses and efferent pathways from the insular cortex in the rat. J Comp Neurol 1991;303:355–374. [PubMed: 2007654]

Zhang Z, Oppenheimer SM. Characterization, distribution and lateralization of baroreceptor-related neurons in the rat insular cortex. Brain Res 1997;760:243–250. [PubMed: 9237541]

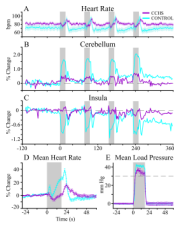

Figure 1.

A: Heart rate during four consecutive Valsalva challenge periods (gray vertical bars, 17.5 s each) in 9 CCHS and 25 control subjects. Shading of traces indicates standard deviation. **B-C:** Mean signal time trends in percent change relative to baseline period (time < 0 s) for CCHS and control subjects during four Valsalva challenge periods in B, ventral cerebellum and C, insular cortex. Averaged trends of **D:** mean heart rate, and **E:** mean load pressure over all four trials in CCHS and control subjects, with error bars indicating standard error of mean (based on RMANOVA). Gray dotted line represents minimum acceptable load pressure for the challenge.

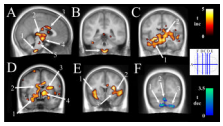

Figure 2.

Cluster analysis: regions of increased (warm colors) or decreased (cool colors) fMRI signal changes during the Valsalva maneuver in CCHS relative to controls (boxcar model). **A:** 1 medulla, including ventrolateral medulla (VLM) and raphé nuclei (magnus, obscurus, pallidus), 2 dorsal midbrain, 3 mid-cingulate, 4 hypothalamus, extending to midbrain, including ventral tegmental area (VTA), 5 mid-pons, **B:** 1 pons, **C:** 1 hippocampus, extending medially to septum, 2 thalamus, extending laterally to basal ganglia, **D:** 1 amygdala, 2 head of caudate, extending to cingulate, 3 internal capsule, extending laterally to putamen and right insular cortex, 4 globus pallidus, **E:** 1 left insula, 2 claustrum, 3 right putamen, extending laterally to cortex, **F:** 1&3 left and right ventral cerebellum, and 2 midline cerebellar cortex. Color scales indicate statistical significance (t statistic) of increasing (inc, warm colors) or decreasing (dec, cool colors) signal differences in CCHS relative to controls. Slice locations (right inset) are in MNI space. A: x = +4 mm, B: y = −40 mm, C: y = −14 mm, D: y = −2 mm, E: y = +14 mm, F: y = −78 mm.

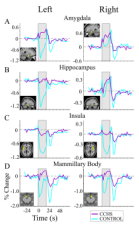

Figure 3.
Rostral/limbic brain areas. Mean signal time trends for 9 CCHS subjects and 25 controls averaged over four Valsalva challenge periods, 17.5 s each. Signals are in percent change relative to baseline. Inset panels show the VOI corresponding to each mean signal time trend.

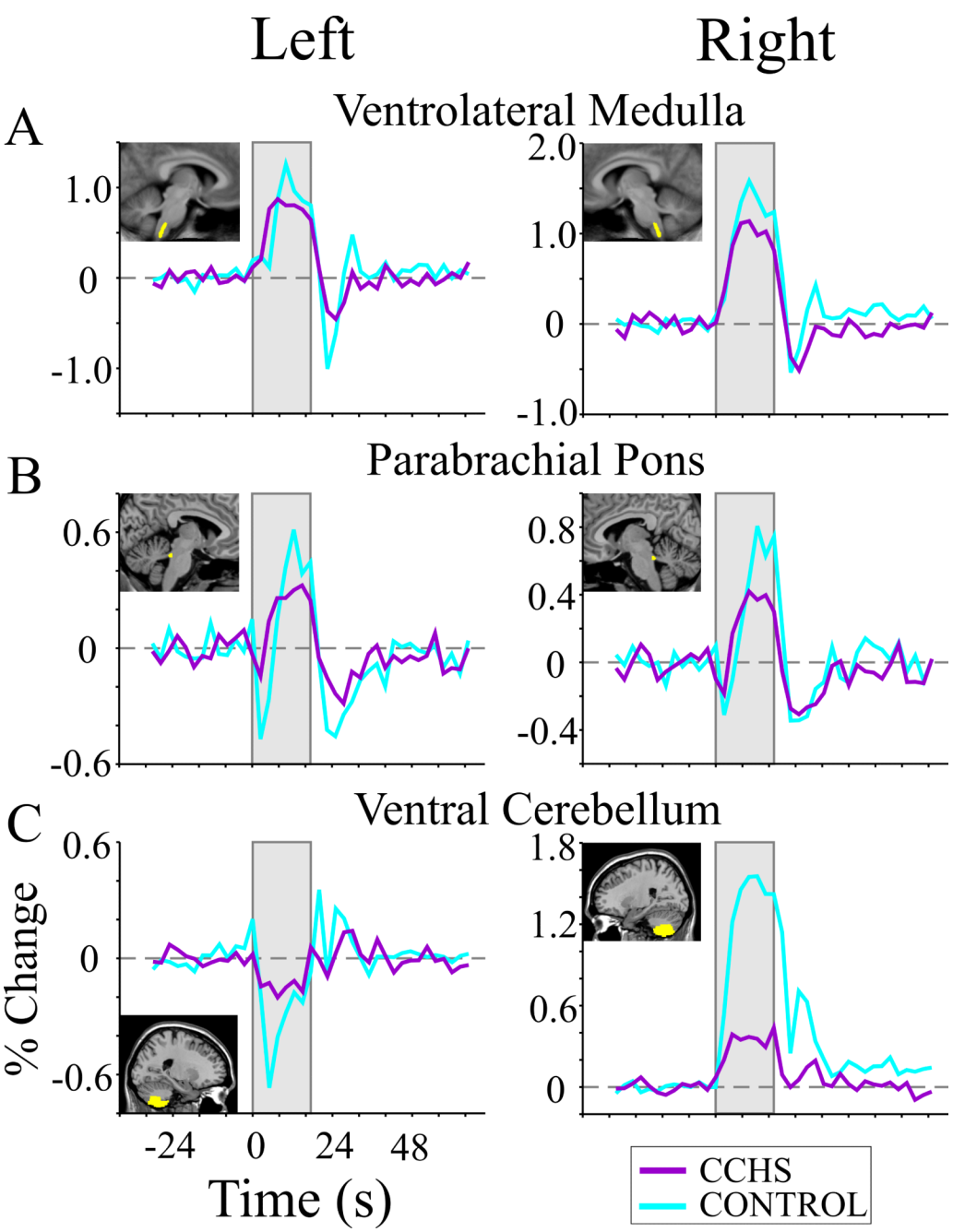

Figure 4.
Caudal brain areas. Mean signal time trends for 9 CCHS subjects and 25 controls averaged over four Valsalva challenge periods, 17.5 s each. Panel characteristics are as in Figure 3.

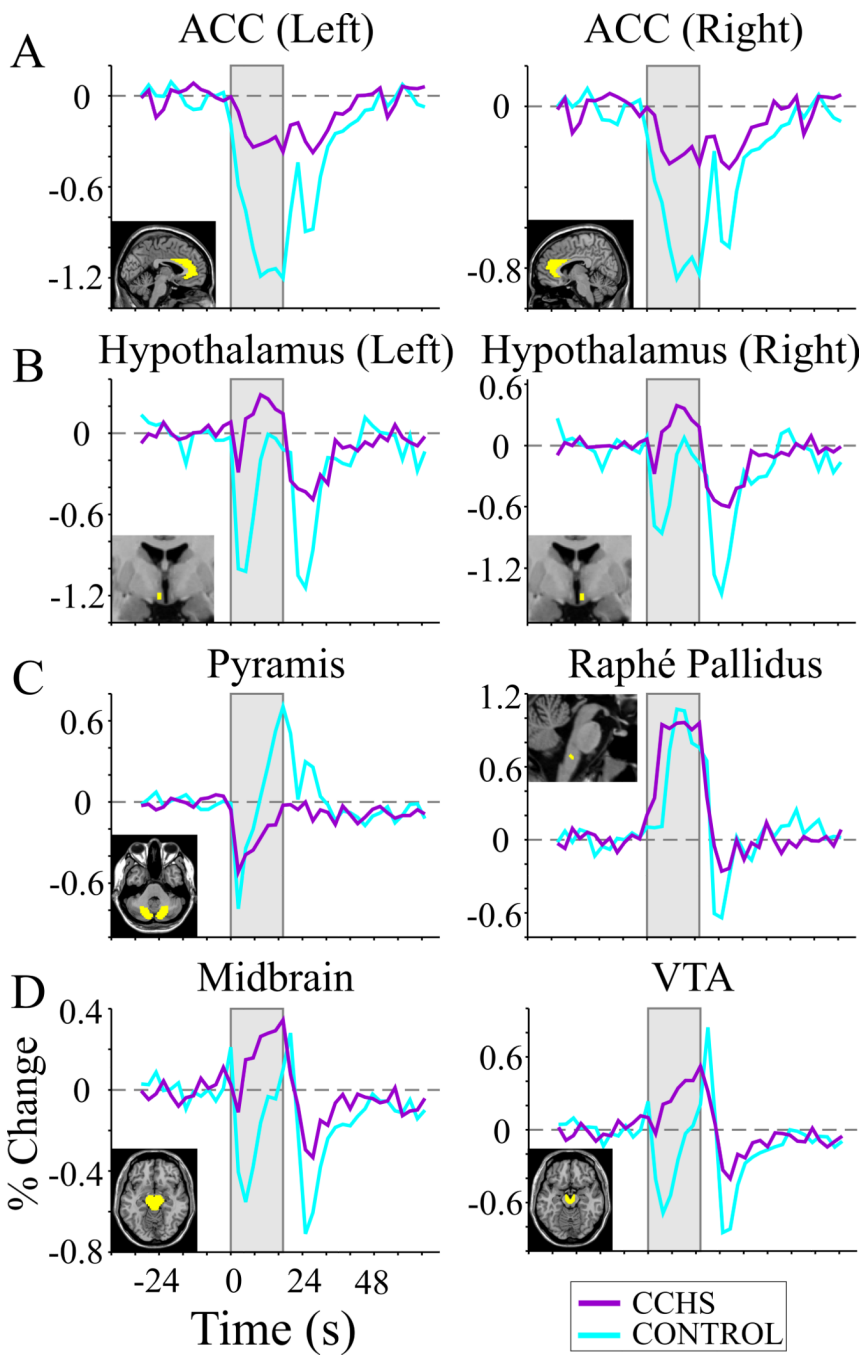

Figure 5.

Timing differences. Mean signal time trends for areas with especially marked phase-lags (ACC, pyramis) and phase-leads (hypothalamus, raphé pallidus, midbrain, VTA); 9 CCHS subjects and 25 controls averaged over four Valsalva challenge periods, 17.5 s each; ACC = anterior cingulate cortex; VTA = ventral tegmental area. Panel characteristics are as in Figure 3.